

# Mandibular Development in *Australopithecus robustus*

Zachary Cofran\*

*School of Humanities and Social Sciences, Nazarbayev University, 53 Kabanbay Batyr Avenue, 010000 Astana, Kazakhstan*

**KEY WORDS** mandible; resampling; growth; allometry

**ABSTRACT** *Australopithecus robustus* has a distinct mandibular anatomy, with a broad and deep corpus and a tall, relatively upright ramus. How this anatomy arose through development is unknown, as gross mandibular size and shape change have not been thoroughly examined quantitatively in this species. Herein, I investigate *A. robustus* mandibular growth by comparing its ontogenetic series with a sample of recent humans, examining age-related size variation in 28 linear measurements. Resampling is used to compare the amount of proportional size change occurring between tooth eruption stages in the small and fragmentary *A. robustus* sample, with that of a more complete human skeletal population. Ontogenetic allometry of corpus robusticity is also assessed with least squares regression. Results show that nearly all measurements experience greater aver-

age increase in *A. robustus* than in humans. Most notably, *A. robustus* corpus breadth undergoes a spurt of growth before eruption of  $M_1$ , likely due in part to delayed resorption of the ramus root on the lateral corpus. Between the occlusion of  $M_1$  and  $M_2$ , nearly all dimensions experience greater proportional size change in *A. robustus*. Nested resampling analysis affirms that this pattern of growth differences between species is biologically significant, and not a mere byproduct of the fossil sample size. Some species differences are likely a function of postcanine megadontia in *A. robustus*, although the causes of other differences are less clear. This study demonstrates an important role of the postnatal period for mandibular shape development in this species. *Am J Phys Anthropol* 000:000–000, 2014. © 2014 Wiley Periodicals, Inc.

This study investigates the developmental basis of mandibular size and shape in *Australopithecus robustus*. This anatomy has generally been interpreted in adaptive terms, as capable of producing and withstanding large masticatory forces (Robinson, 1954; Rak, 1983; Wolpoff, 1999; Teaford and Ungar, 2000; Grine et al., 2012). Tall mandibular rami provide a lever advantage to the medial pterygoid and to the masseter muscles which close the jaw, facilitating largely vertical chewing forces (Rak and Hylander, 2008). Tall rami also reduce gape, resulting in more evenly distributed occlusal forces throughout the length of the tooth row.

Consistent with powerful chewing capabilities, mechanical properties of the *A. robustus* bony mandible theoretically allow it to withstand such high stresses (Wolpoff, 1975; White, 1977). For instance, the ramus is strengthened against vertical bending forces from the temporalis muscle by a pronounced endocoronoid buttress. The mandibular symphysis is buttressed medially with superior and inferior “tori,” keeping the symphysis from wishboning during mastication. More distally, the corpus is resistant to transverse bending and torsion forces due to the distribution of cortical bone about a relatively broad (“robust”) cross-section (Daegling, 1989; Daegling and Grine, 1991; Grine and Daegling, 1993). Indeed, the adult *A. robustus* corpus is much broader than expected for a hominoid of its estimated body size (Wood and Aiello, 1998) and has been described as “overdesigned” to withstand high masticatory stresses (Daegling and Hylander, 2000: 548). Whether robust gross anatomy is present early in life or arises later during growth has yet to be determined.

Despite a relatively large ontogenetic series, mandibular growth and development have not been fully analyzed for *A. robustus* (see Lockwood et al., 2007 for analysis of facial growth after adulthood). At the micro-

scopic level, Bromage (1989) and McCollum (2008; maxillae only) compared the distribution of bony remodeling fields in the face of fossil hominins, humans and chimpanzees. These authors found similar patterns of periosteal remodeling between *A. robustus* and modern humans, shared to the exclusion of “gracile” australopiths and early *Homo*. For example, the anterior surface of the mandible is usually largely depository throughout ontogeny in chimpanzees (Johnson et al., 1976) and non-robust hominins (Bromage, 1989), reflecting prognathism and predominantly forward direction of facial growth in these species. Contrarily, the anterior alveolar surface is fully resorptive in humans (Enlow and Harris, 1964), and in *A. robustus* this surface is depository medially but resorptive laterally (Bromage, 1989). Similarly reflecting an orthognathic face, humans and *A. robustus* share relatively early fusion of the premaxillary suture to the exclusion of apes and gracile australopiths (Braga, 1998). Such facial similarities between these species, such as a parabolic dental arch and a short face, may thus be underlain by similar processes of growth and development.

Grant sponsor: University of Michigan International Institute, Center for African Studies.

\*Correspondence to: Zachary Cofran, School of Humanities and Social Sciences, Nazarbayev University, 53 Kabanbay Batyr Avenue, Astana, Kazakhstan. E-mail: zachary.cofran@nu.edu.kz

Received 3 October 2013; accepted 23 April 2014

DOI: 10.1002/ajpa.22527  
Published online 00 Month 2014 in Wiley Online Library (wileyonlinelibrary.com).

At the same time, however, anatomical differences between humans and *A. robustus* have led Bromage (1989) and McCollum (1997, 1999) to hypothesize differences in facial growth. During the ontogeny of humans and apes, the height of the posterior face increases more than the front, resulting in the apparent rotation of the mandible relative to the cranial base (Björk and Skieller, 1972; Wang et al., 2009). Because the adult *A. robustus* posterior face (i.e., ascending ramus) is vertically tall, Bromage (1989) and McCollum (1997, 1999) have reasoned that *A. robustus* likely experienced greater anterior facial rotation during postnatal ontogeny than do humans. Alternatively, a relatively tall posterior face may have been established by birth in this species, with a comparable degree of rotation as found in other apes postnatally. Similarly, the robust corpus of this species could be a characteristic that is present in the youngest infants, or the robust corpus may come about later during postnatal growth.

Many studies have investigated whether morphological differences between hominoid and hominin faces are the result of either different ontogenetic starting points (established prenatally) following similar growth trajectories, or more divergent ontogenetic trajectories between species (e.g., Shea, 1983; Richtsmeier and Walker, 1993; Ackermann and Krovitz, 2002; Cobb and O'Higgins, 2004; Zollikofer and Ponce de León, 2004; McNulty et al., 2006; Gunz, 2012). Such analyses usually examine multivariate datasets, which can only be statistically analyzed in samples with no missing data. As a result, most of these studies have rarely included more than one non-adult fossil, which both overlooks many stages of the growth period and underestimates intraspecific variation at a given developmental stage.

The relatively large *A. robustus* mandibular sample is uniquely suited among early hominins to examine the development of size and shape, and to test the null hypothesis that this species follows a similar trajectory of size/shape change as humans. At no stage of development do *A. robustus* and human mandibles look identical, indicating an important role for early, possibly prenatal, development in establishing species morphology. Indeed, many comparative studies of hominoid facial development have found that anatomical differences between adults of different species, or even populations of the same species, are present at early postnatal ages (e.g., Daegling, 1996; Ponce de León and Zollikofer, 2001; Ackermann and Krovitz, 2002; Strand Viðarsdóttir et al., 2002; Mitteroecker et al., 2004; Zollikofer and Ponce de León, 2004; McNulty et al., 2006; Fukase and Suwa, 2008). Basicranial variation between extant hominoids seems also to be established largely before rather than after birth (Dean, 1988b).

Rejection of the hypothesis of similar postnatal growth patterns between humans and *A. robustus* may also be expected, however, as dietary consistency has been shown to influence mandibular development, as bone responds adaptively to hard versus soft diets (Lieberman et al., 2004; Holmes and Ruff, 2011). *A. robustus* likely had a much harder diet than recent humans (reviewed in Grine et al., 2012), and so it is also possible that its distinct anatomy (i.e., corpus robusticity) arose during postnatal growth. This study therefore seeks to elucidate how and why the *A. robustus* mandible assumes its unique adult shape. It should be noted that the focus here is on hemi-mandibular rather than on complete mandibular shape per se, as constrained by fossil preser-

vation. This necessary focus obfuscates the interesting similarity in dental arcade shape between humans and *A. robustus* at all ages (Skinner, 1978, cited in Dean et al., 1993). Nevertheless, it is the goal of this study to ascertain as much about *A. robustus* mandibular growth as is possible despite poor preservation.

Herein, I present a computationally intense randomization procedure to compare patterns of relative size change in mandibles of humans and *A. robustus*. A randomization approach is necessary since it accommodates the problem of pervasively missing data in the fossil sample. A heterochronic framework for the comparison of growth (e.g., Williams et al., 2003) is not employed here, as heterochrony requires an ancestral growth pattern or trajectory be known or identified (Alberch et al., 1979; McNulty, 2012); both humans and *A. robustus* show quite derived anatomies relative to earlier hominins, and so each is an inappropriate model for the ancestral condition of development. Although heterochrony is not directly addressed, I do compare corpus height and breadth ontogenetic allometries at the positions of P<sub>4</sub> and M<sub>1</sub>, as these are well represented in both species. Comparison is only with modern humans for several reasons: first, humans are the closest living relatives of *A. robustus*, and the two species share the same sequence of dental eruption (Smith, 1986). Second, because hominoid species have been shown to follow their own patterns of craniofacial size/shape growth (Cobb and O'Higgins, 2004; Mitteroecker et al., 2004, 2005), simultaneous comparisons of *A. robustus* with other ape taxa may not be clearly interpreted, whereas a single species comparison may more easily contextualize size and shape change in the fossil species. Finally, other fossil hominins are not included because their ontogenetic sample sizes are inferior to those of *A. robustus*.

## MATERIALS AND METHODS

### Samples

The *A. robustus* mandibular sample utilized here comprises 13 individuals from the Early Pleistocene site of Swartkrans (Pickering et al., 2011), ranging in age from infancy to late adolescence, with several specimens at similar stages of dental development (Table 1). This sample is thus capable of providing some evidence of variation within and between age groups, avoiding the challenge posed by many fossil studies of development. Because of elevated sexual dimorphism in adults of this species (Lockwood et al., 2007), only non-adults (i.e., before occlusion of M<sub>3</sub>) are considered. The human sample ( $n = 122$ ) is from the site of Libben in Ohio, dating to between 800–1100 CE (Lovejoy et al., 1977). This sample is ideal for comparison with a fossil taxon because it is large, pre-agricultural and healthy, and temporally restricted (Meindl et al., 2008).

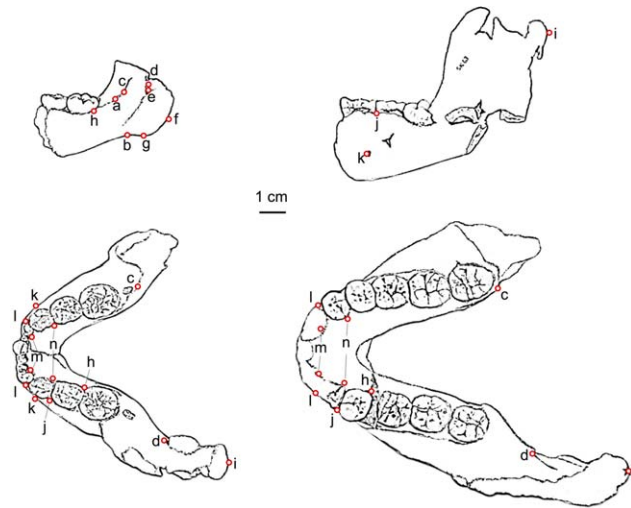
It is improbable that sex can be reliably determined from non-adult mandibles, especially for extinct species. Thus, although sexual dimorphism is a potential source of variation in this ontogenetic study, each species is treated as a single, non-sexed sample. Specimens are assigned to one of five dental eruption stages (Table 1). Stages distinguishing erupting vs. occluded teeth (e.g., McNulty et al., 2006; McNulty, 2012) were selected to maximize the number of age groups in the fossil dataset. Although there is a large amount of intra- and inter-population variation in the chronological ages at which these stages are attained (Dahlberg and Menegaz-Bock,

TABLE 1. Definition of eruption stages and specification of samples<sup>a</sup>

Eruption stage	<i>A. robustus</i>	Humans ( <i>n</i> )
1: Deciduous $m_2$ erupting/occluded	SK 64, 438, 3978	36
2: $M_1/I_1$ erupting but not in occlusion	SK 61, 62	10
3: $M_1$ occluded but $M_2$ unerupted/unoccluded	SK 63	32
4: $M_2$ occluded but $M_3$ unerupted	SK 6, 25, 55b, 843 <sup>b</sup> , 1587 <sup>b</sup> , SKX 4446	33
5: $M_3$ erupting but not occluded	SKW 5	11
Total	13	122

<sup>a</sup>Specimen numbers are given for *A. robustus* but only sample sizes are given for humans.

<sup>b</sup>These specimens each preserve only one measurable variable (SK 843 = corpus height at  $P_4/M_1$ , SK 1587 = corpus breadth at  $M_1$ ).



**Fig. 1.** Landmarks used to define non-standard measurements defined in Table 2. Scale bar is 1 cm. Top left: SK 64 (eruption Stage 1) viewed medially. Top right: SK 63 (eruption Stage 3) viewed laterally. Bottom left: SK 63 right and left halves. Bottom right: SKW 5 (eruption Stage 5). Note that bilateral mandibular breadths (Measurements 23–26) were not taken from the broken SK 63, and Measurements 24–25 (l-l and m-m) were estimated for SKW 5. [Color figure can be viewed in the online issue, which is available at [wileyonlinelibrary.com](http://wileyonlinelibrary.com).]

1958; Wolpoff, 1979; Hägg and Taranger, 1981; Eveleth and Tanner, 1988; Tompkins, 1996; Liversidge, 2003), eruption sequence is comparable between populations and arguably more closely related to the growth process and life history. Thus, these stages may be considered developmentally homologous between these species, although they do not necessarily imply the same chronological ages or time spans between eruptions (see, for example, LaCruz et al., 2008).

Up to 28 linear measurements that describe mandibular size and shape (Fig. 1 and Table 2) were taken on each mandible, depending on individual preservation. Variables were selected to maximize information obtainable from the fossil sample. These traits can be broadly divided into five categories: 1) breadth and 2) height of the corpus and symphysis, 3) anteroposterior mandibular length, 4) anterior, bilateral mandibular breadth, and 5) ramus height and anteroposterior length. Where possible, only an individual's left side was measured, although data from the right side were used if unavailable on the left. In a few instances where a fossil did not preserve a trait but the measurement could be reliably

and repeatably estimated, this estimate was used (e.g., symphysis height for SKW 5).

Measurements were taken to the nearest 0.1 mm with digital sliding calipers. To assess measurement error, each of the 28 measurements was taken three times on each fossil, and on a subset ( $n = 48$ ) of the humans encompassing all eruption stages. Most measurements differed by 0.0–0.2 mm between replications, and the difference between the maximum and minimum triplicates rarely (<1% of the time) exceeded 1.00 mm. For the fossils and this subset of individuals, the average value of the replications was used in the analysis.

### Comparing patterns of size change

Fossil samples present many challenges to the comparative analysis of growth, age-related variation in size. Most notably, mandibular shape is a multivariate issue, and multivariate statistics require large samples without missing data. Fossil samples, however, are generally small and poorly preserved, and specimens do not always preserve homologous features (e.g., Figs. 1–2). The *A. robustus* mandibular ontogenetic series is large and complete by fossil standards, and so can potentially reveal much about growth in this species, but this cannot be assessed with traditional statistical methods.

Rather than attempting to see whether humans and *A. robustus* follow similar trajectories through multivariate space (e.g., Cobb and O'Higgins, 2004), randomized resampling statistics are used to rephrase the question: what are the chances of seeing the pattern of variation observed in the fossil sample, in a larger and better preserved cross-sectional sample? Randomization has the benefit of being free of distributional assumptions (Manly, 2007; Mattfeldt, 2011), and it alone allows fragmentary specimens to be included. The question posed above is addressed by randomly sampling pairs of humans and fossils in the same eruption stages, to assess whether each pair undergoes comparable relative size change between stages for a given measurement. Repeated resampling thus creates an empirical estimation of the probability of seeing the same amount of size change for each trait in both species.

Growth in each trait is measured as the proportional size change that occurs between different dental stages, similar to the approach taken in Euclidean Distance Matrix Analysis (EDMA; Richtsmeier and Lele, 1993). Whereas EDMA relies on complete specimens and “form matrices,” the present algorithm simply compares pairs of specimens for whichever traits they share in common, individually. A proportion, rather than an absolute difference, to describe size change between stages in each species is necessary as the *A. robustus* mandible ultimately reaches a larger size than human jaws. It should

TABLE 2. Description of measurements

Trait number	
	<i>Corpus breadth: buccal-lingual width of the corpus paralleling the vertical long axis at a given position</i>
1	Breadth at P <sub>3</sub>
2	Breadth at the P <sub>3-4</sub> septum
3	Breadth at P <sub>4</sub>
4	Breadth at the P <sub>4</sub> -M <sub>1</sub> septum
5	Breadth at M <sub>1</sub>
6	Breadth at the M <sub>1</sub> -M <sub>2</sub> septum
7	Breadth at M <sub>2</sub>
8	Breadth at the symphysis
	<i>Corpus height: perpendicular distance from the corpus base to the buccal alveolar margin, at a tooth midpoint or at the septum between two teeth (9-14)</i>
9	Height at the P <sub>3-4</sub> septum
10	Height at P <sub>4</sub>
11	Height at the P <sub>4</sub> -M <sub>1</sub> septum
12	Height at M <sub>1</sub>
13	Height at the M <sub>1-2</sub> septum
14	Height at M <sub>2</sub>
15	Height from the center of the mental foramen to the corpus base
16	Distance from the center of the mental foramen to the nearest point on alveolar margin
17	Lingual tuberosity height: perpendicular height from the basal ramus-corporum junction to the lingual alveolar margin (a-b) <sup>a</sup>
18	Height from the base of the symphysis to infradentale
	<i>Anteroposterior mandibular length</i>
19	Distance from the buccal P <sub>4</sub> -M <sub>1</sub> septum to infradentale
20	Maximum distance from the posterior condylar surface to the lingual I <sub>2</sub> -C septum (i-m) <sup>a</sup>
21	Distance from the center of the mental foramen to the posteromedial margin of the superior surface of the lingual tuberosity, before it rises vertically as the endocoronoid ridge or buttress (k-c) <sup>a</sup>
22	Distance from the anterior margin of the mandibular foramen to the lingual P <sub>4</sub> -M <sub>1</sub> septum (d-h) <sup>a</sup>
	<i>Bilateral anterior mandibular breadth</i>
23	Minimum distance between the mental foramina (k-k)
24	Maximum distance between the buccal canine alveolus margins (l-l)
25	Minimum distance between the lingual canine alveolus margins (m-m)
26	Distance between the distal-lingual corner of the P <sub>3</sub> alveolus margins (n-n)
	<i>Ramus height and anteroposterior length</i>
27	Distance from the posterior ramus margin on the alveolar plane to the buccal P <sub>3-4</sub> septum (f-j) <sup>a</sup>
28	Perpendicular distance from the inferior ramus margin to the mandibular foramen (g-e) <sup>a</sup>

Measurements involving the permanent P<sub>3-4</sub> correspond to the deciduous teeth they replace (dm<sub>1-2</sub>, respectively) in juveniles.

<sup>a</sup> Lettered landmark coordinates for non-standard measurements are illustrated in Figure 1.

be stressed that this study does not calculate and compare growth rates per se, i.e., as absolute size changes between specified chronological ages, because such ages cannot be reliably estimated for the majority of the fossil sample.

The following algorithm is used to test whether humans and *A. robustus* can be distinguished in terms of patterns of relative size change for each mandibular measurement:

1. Randomly select two *A. robustus* mandibles in different eruption stages, and then randomly select two human mandibles matching the fossils' stages.
2. Randomly select one of the traits these two pairs of specimens share in common. If no traits are shared between all four specimens, Step 1 is repeated until a set of specimens can be compared.
3. Calculate a test statistic, *grdif* ("growth difference"), describing the *species difference* in the amount of relative change in size between the eruption stages:

$$\text{grdif} = \left[ \left( \frac{\mathbf{R}}{\mathbf{Y}} \right) - \left( \frac{\mathbf{H}}{\mathbf{Y}} \right) \right]$$

where *R* and *H* denote *A. robustus* and human specimens, respectively. A cross-sectional sample raises the possibility of sampling older individuals that are

"unrealistically" smaller than younger ones; here, if the older individual in a pair is smaller than the younger, the species' growth ratio (but not *grdif*) is set to 1 indicating no size change. As the absolute difference between two ratios, *grdif* = 0 means no difference in proportional size change, while positive values indicate that *A. robustus* underwent greater relative size change in this comparison, and negative values the opposite.

4. Repeat this resampling 300,000 times, to obtain a distribution of *grdif* values for each trait. This large number of iterations ensures that as many pairwise comparisons made are made as possible; to reduce redundancy, *grdif* statistics based on the same interspecific comparisons for any trait are included only once.

If *grdif* = 0 is outside the range of the majority of resampled values, there may be statistically sufficient grounds to reject the null hypothesis in favor of an alternate hypothesis of different patterns of size-change between species. *P* values are presented in terms of the proportion of comparisons in which a human pair undergoes at least as much size change as the *A. robustus* pair; for instance, if 10% of all comparisons for a trait indicate more size change in humans, then *P* = 0.10.

TABLE 3. Summary of *grdif* statistics for each trait, for all pairwise eruption stage comparisons

Trait ID	<i>n</i>	Mean <i>grdif</i>	Minimum, maximum	95% quantiles	<i>P</i> value
All traits	109,051	0.254	-1.131, 1.833	-0.290, 0.888	0.189
1	4,509	0.362	-0.402, 0.927	-0.081, 0.927	0.081
2	4,959	0.311	-0.488, 0.793	-0.096, 0.793	0.114
3	11,282	0.277	-0.531, 0.561	-0.069, 0.561	0.082
4	9,761	0.242	-0.370, 0.520	-0.085, 0.520	0.125
5	8,541	0.228	-0.043, 0.648	-0.073, 0.601	0.067
6	896	0.105	-0.382, 0.203	-0.144, 0.203	0.123
7	677	0.102	-0.233, 0.332	-0.123, 0.331	0.440
8	1,297	0.280	-0.354, 0.990	-0.150, 0.802	0.181
9	7,690	0.201	-0.494, 0.982	-0.259, 0.761	0.252
10	11,904	0.352	-0.681, 1.33	-0.235, 1.06	0.161
11	10,525	0.269	-0.744, 1.06	-0.291, 0.780	0.205
12	5,398	0.158	-0.760, 0.892	-0.343, 0.636	0.284
13	1,081	-0.111	-0.676, 0.218	-0.464, 0.218	0.834
14	736	-0.159	-0.739, 0.025	-0.497, 0.025	0.861
15	10,019	0.156	-1.12, 1.09	-0.532, 0.882	0.330
16	5,652	0.202	-1.13, 1.056	-0.494, 0.945	0.332
17	4,556	0.295	-0.525, 1.00	-0.250, 0.888	0.170
18	282	0.133	-0.290, 0.428	-0.181, 0.376	0.199
19	104	0.022	-0.134, 0.055	-0.113, 0.055	0.173
20	14	0.211	0.070, 0.347	0.084, 0.332	0
21	2,481	0.282	-0.251, 0.767	-0.102, 0.671	0.100
22	5,036	0.401	-1.00, 1.83	-0.378, 1.44	0.152
23	327	0.244	-0.245, 0.585	-0.178, 0.525	0.187
24	84	0.112	-0.261, 0.348	-0.185, 0.238	0.119
25	124	0.259	-0.243, 0.508	-0.115, 0.507	0.065
26	172	0.084	-0.357, 0.236	-0.248, 0.236	0.291
27	258	0.399	-0.196, 1.06	-0.151, 1.00	0.127
28	686	0.396	-0.439, 0.899	-0.124, 0.899	0.071

This approach essentially tests multiple univariate hypotheses at once, comparing species for proportional size change in several traits between many combinations of dental eruption stages. The question then arises whether the thousands of resulting *grdif* statistics reflect a biologically meaningful pattern of difference between species. A post hoc “nested resampling” procedure (Van Arsdale, 2006; Van Arsdale and Lordkipanidze, 2012) is used to test whether the observed distribution of *grdif* is unexpected under the null hypothesis of indistinguishable patterns of growth between species. A new test statistic, “T4” (calculation described in Results), quantifies the observed distribution of *grdif* across subsequent eruption stages (i.e., 1–2, 2–3, 3–4, and 4–5). Nested resampling involves repeating the *grdif* analysis on the human sample alone, to assess the likelihood of observing the empirical T4 value. First, divide the human sample into a subset of 13 specimens matching the fossils in sample size and eruption stages, and the remaining 109 continuing to represent humans. Next, run the original *grdif* algorithm, resampling 5,000 *grdif* with these subsamples, and then calculate the T4 statistic. Sample division, *grdif* analysis and T4 calculation are repeated 500 times to create a T4 distribution determining whether the observed fossil-human comparison is extreme. All analyses are written in R (R Core Team, 2013), and are available from the author on request.

The randomization test examines individual measurements, and not shapes or ratios. Corpus breadths and heights are well represented in the *A. robustus* sample, allowing a comparison of corpus robusticity between this hominin and humans. Most hominoid corpora have a relatively circular cross-section in infancy (Dean, 1988a; personal observation), but the *A. robustus* mandible remains relatively broad into adulthood compared with

other hominoids (Daegling and Grine, 1991; Wood and Aiello, 1998). To investigate the development of robusticity, I also compare the ontogenetic allometry of corpus height and breadth at the P<sub>4</sub> and M<sub>1</sub> positions between species, with least squares regression.

## RESULTS

Most traits undergo greater size change in *A. robustus* compared with humans (Table 3). If we consider all resampled combinations of specimens, all but two traits have an average *grdif* greater than 0, indicating greater size change in *A. robustus*. None of these is statistically significant at the  $P \leq 0.05$  level, although a few are significant at  $P \leq 0.10$  (Figs. 2–4): corpus breadth at P<sub>3</sub>, P<sub>4</sub>, and at M<sub>1</sub> (traits 1, 3, and 5), length from the mental foramen to the lingual tuberosity (trait 21), internal bicanine breadth (Trait 25), and ramus height from the mandibular foramen (trait 28). Humans never undergo as much size increase from the posterior condyle to the lingual I<sub>2</sub>-C alveolar septum (Trait 20), a rough measure of overall mandibular length. On the one hand, this should be viewed with caution since poor sample preservation means this was based on only 14 comparisons, of specimens in eruption Stages 3–5 only. On the other hand, this dimension is likely underestimated for SKW 5, whose superior-most ramus and condyle are largely missing. In short, then, the overall results of the *grdif* analysis confirm what is easily discernible with the naked eye, that although *A. robustus* and human mandibles are similar in size at early stages, the former reaches attains a much larger size by adulthood.

The subset of “nearly significant” ( $P \leq 0.10$ ) traits indicates that major shape differences between human and *A. robustus* mandibles arise from postnatal growth

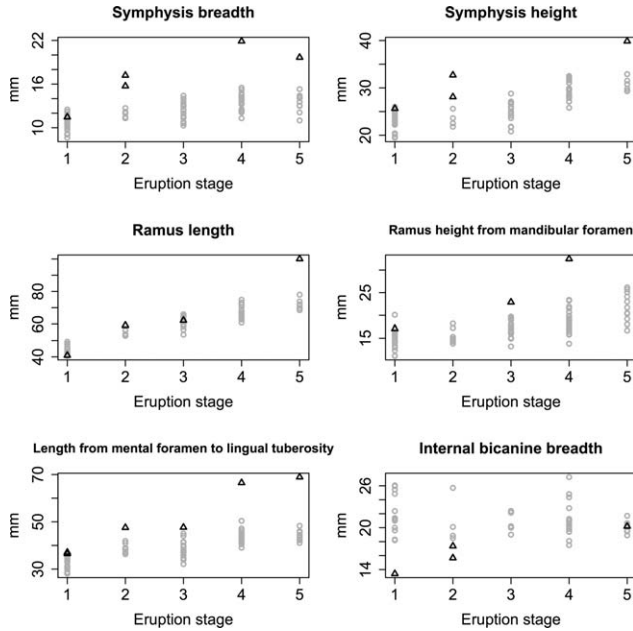


**Fig. 2.** Raw data plotted against dental eruption stage for select measurements. Humans are circles and *A. robustus* are triangles. Plots further highlight the problem of missing data and disparate specimen preservation in the fossil sample.

differences in corpus breadth, posterior corpus length, anterior mandibular breadth, and posterior facial height. These could all be expected from the respective facts that *A. robustus* has thicker corpora, a more prognathic face due in part to longer postcanine teeth, smaller canines, and a taller posterior face. The only traits with a negative average *grdif* (i.e., humans usually undergo more size change) are corpus heights between M<sub>1-2</sub> and at M<sub>2</sub> (Traits 13–14), but these are not significant and only comprise individuals in eruption Stages 4–5. Indeed, the timing of these interspecific growth differences becomes apparent when examining *grdifs* between subsequent age groups ( $n = 38,264$  pairwise comparisons; Table 4).

### Eruption stages 1–2

Between the earliest eruption stages, mean *grdif* = 0.139, and *grdif* ≤ 0 for 19.3% of 10,501 pairwise comparisons (Table 4): in other words, the majority of pairwise comparisons indicate greater proportional size change in *A. robustus*. Most measures of corpus breadth and bilateral anterior mandibular breadth undergo significantly greater size increase in *A. robustus*. In addition, the ramus elongates more in *A. robustus*, although this is based on only 48 pairwise comparisons (Trait 27). In contrast, although *A. robustus* experiences greater corpus and ramus height growth on average during this time, it is not uncommon to see at least as much change in the human sample. Similarly, although relatively

**TABLE 4.** *Grdif* statistics for each trait between successive eruption stages

Trait	Period 1–2		Period 2–3		Period 3–4		Period 4–5	
	Mean <sup>a</sup>	<i>P</i> ( <i>n</i> )	Mean	<i>P</i> ( <i>n</i> )	Mean	<i>P</i> ( <i>n</i> )	Mean	<i>P</i> ( <i>n</i> )
All traits	0.139	0.193 (10,501)	−0.053	0.558 (3,647)	0.244	0.085 (13,221)	−0.048	0.728 (10,895)
1	<b>0.304</b>	0 (930)	−0.021	0.368 (365)	<b>0.261</b>	0.011 (281)	<b>−0.053</b>	1 (191)
2	<b>0.247</b>	0.007 (907)	−0.040	0.725 (411)	<b>0.258</b>	0.012 (396)	<b>−0.052</b>	1 (213)
3	0.112	0.073 (1,675)	−0.022	0.353 (476)	<b>0.231</b>	0.023 (863)	<b>−0.048</b>	1 (489)
4	0.062	0.275 (1,438)					<b>−0.025</b>	1 (767)
5	<b>0.147</b>	0.030 (436)	0.043	0.190 (210)	0.029	0.270 (1,342)	0.120	0.053 (756)
6					0.105	0.123 (896)		
7							0.101	0.440 (677)
8	<b>0.315</b>	0.021 (291)					<b>−0.052</b>	1 (146)
9	0.048	0.392 (564)	−0.070	0.651 (281)	0.248	0.080 (1,126)	−0.083	0.846 (729)
10	0.095	0.317 (1,006)	−0.045	0.588 (362)	<b>0.319</b>	0.020 (1,372)	<b>−0.131</b>	0.962 (679)
11	−0.070	0.629 (642)	−0.001	0.411 (387)	<b>0.333</b>	0.026 (1,823)	−0.127	0.946 (905)
12			−0.051	0.519 (376)	0.251	0.105 (1,644)	−0.095	0.733 (1,004)
13							−0.111	0.834 (1,081)
14							−0.159	0.861 (736)
15	0.120	0.317 (961)	−0.182	0.837 (484)	0.274	0.119 (1,330)	0.028	0.489 (767)
16	0.222	0.230 (513)					<b>−0.141</b>	1 (638)
17	0.181	0.101 (328)	<b>−0.128</b>	1 (134)	0.346	0.055 (488)	0.063	0.356 (407)
18	0.127	0.171 (117)						
19	0.019	0.209 (43)						
20								
21	0.126	0.162 (284)	−0.042	0.553 (132)	<b>0.270</b>	0.005 (219)	0.002	0.333 (198)
22					0.264	0.068 (1,225)	0.045	0.330 (512)
23	<b>0.361</b>	0 (163)						
24	<b>0.121</b>	0 (31)						
25	0.188	0.137 (51)						
26	<b>0.181</b>	0 (73)						
27	<b>0.251</b>	0 (48)	−0.094	0.897 (29)				
28					0.276	0.083 (216)		

<sup>a</sup> Empty cells mean no comparisons could be resampled for a given trait between successive eruption stages. Bold values indicate that less than 5% the resampled distribution is less than or equal to 0 (i.e.,  $P \leq 0.05$ , *A. robustus* undergoes greater size change), or conversely that less than 5% of the distribution is greater than or equal to 0 (i.e.,  $P \geq 0.95$ , humans undergo greater size change).

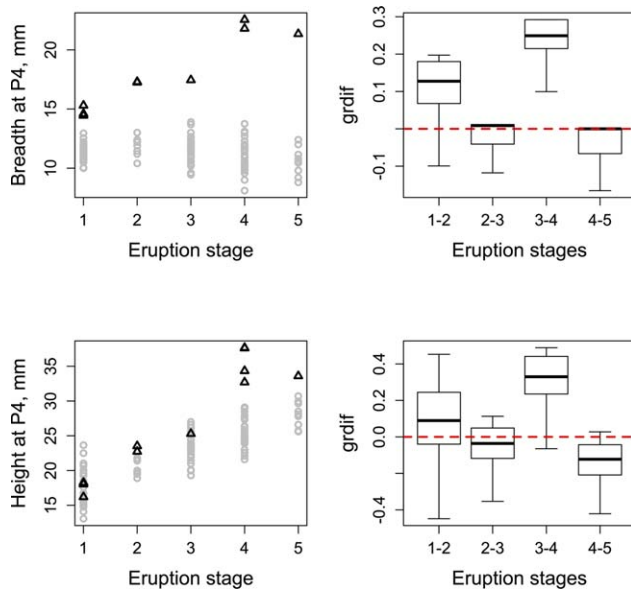


**Fig. 3.** Raw data (left) and the boxplots of the associated grdif statistics (right) for corpus breadth (top) and height (bottom) at P<sub>4</sub>. In the data plots, humans are circles and *A. robustus* are triangles. In the grdif plots, thick black bars in each box indicate the median, boxes comprise the 50% quantiles, lines extend to the minima and maxima, and the dashed line indicates grdif=0 (no difference in proportional size change between species). Note that grdif for breadth at P<sub>4</sub> between eruption Stages 4–5 has a median of 0: this is because Stage 5 individuals are always (*A. robustus*) or often (humans) smaller than those in Stage 4, resulting in each species' growth ratio being set to 1. [Color figure can be viewed in the online issue, which is available at [wileyonlinelibrary.com](http://wileyonlinelibrary.com).]

scantly sampled, growth in anteroposterior corpus lengths (Traits 19 and 21) cannot be distinguished between species. In sum, compared with humans, the *A. robustus* corpus and anterior jaw broaden, and the ascending ramus elongates, more between occlusion of the deciduous dentition and the beginning of M<sub>1</sub>/I<sub>1</sub> eruption.

### Eruption stages 2–3

In contrast to the preceding eruption period, all dimensions undergo greater change in humans on average between M<sub>1</sub> eruption and occlusion, though the species differences are not great. The only trait significantly different is corpus height at the lingual tuberosity (Trait 17, mean grdif = -0.128), for which none of the 134 *A. robustus* pairs show as great proportional size difference as humans. It should be noted that the only *A. robustus* specimen in Stage 3, SK 63, has only slightly advanced states of crown and root formation compared to the two fossils in Stage 2, SK 61 and 62 (Conroy and Vannier, 1991).

### Eruption stages 3–4

Growth is the most distinct between humans and *A. robustus* between the eruptions of M<sub>1-2</sub>. Mean grdif is a relatively high 0.244, and humans match *A. robustus* in size change in fewer than 9% of the 13,221 pairwise comparisons. Fourteen of the 28 traits can be examined between stages 3–4 and  $P \leq 0.10$  for all but four (Traits 5, 6, 12, and 15). Unlike the species difference between

Stages 1–2 in which the main species difference was anterior corpus broadening in *A. robustus*, Period 3–4 sees nearly every part of the *A. robustus* mandible increase relatively more, including corpus and ramus height. Thus, *A. robustus* undergoes greater global size, rather than strictly shape, change than humans during this time.

### Eruption stages 4–5

Finally, between occlusion of M<sub>2</sub> and before full occlusion of M<sub>3</sub>, there is relatively little difference between species in size and shape change. As between eruption Stages 2–3, overall average grdif is negative, but not notably so. Corpus breadths at the symphysis and premolars increase more in humans than *A. robustus* ever does, but the species difference is not great. Posteriorly, however, corpus breadth at the M<sub>1</sub> and M<sub>2</sub> increases more in *A. robustus*; the difference is not significant but is nearly so at M<sub>1</sub>. Three corpus height measures (Traits 10, 11, and 16), undergo a notably greater amount of size change in humans. Most other measures of corpus height have negative average grdifs, but the chance of finding such great size change in *A. robustus* is not as low. Results from this time period must be tempered by the fact that *A. robustus* is represented in eruption Stage 5 only by the relatively short and broad SKW 5 (Grine and Daegling, 1993).

### Nested resampling

An intriguing result is that there is a high average grdif when examining all traits in both Periods 1–2 and 3–4, and a negative but less notable average in the other stages (i.e., first line of Table 4). Many of these individual traits with high average grdifs in Periods 1–2 and 3–4 show low P values but are not quite significant at the traditional threshold. Nevertheless, the clustering of positive and negative grdifs by eruption stage suggests important species differences in patterns of size and shape change, the significance of which can be assessed using nested resampling. The observed pattern is quantified as T4: the sum of mean grdifs for Periods 1–2 and 3–4, minus the sum of the average grdifs for Periods 2–3 and 4–5:

$$T4 = \{[\text{mean}(\text{grdif}_{1-2}) + \text{mean}(\text{grdif}_{3-4})] - [\text{mean}(\text{grdif}_{2-3}) + \text{mean}(\text{grdif}_{4-5})]\}$$

The empirical human-fossil T4 = 0.484. This statistic nicely quantifies the observed pattern, since there are high averages being summed and negative averages being subtracted (i.e., the absolute value added), resulting in a characteristically high value.

The nested resampling analysis results in a normal distribution ( $W = 0.996$ ,  $P = 0.266$ ) of T4 with a mean of -0.005. Only 4/500 resampled test statistics exceed the observed *A. robustus*-human value ( $P = 0.008$ ). Thus, the high average grdifs between humans and *A. robustus* in Periods 1–2 and 3–4, with little or no difference in the other periods, most likely reflects real differences in size and shape change between these species, contributing to their adult mandibular shapes.

### Allometry of corpus robusticity

Plots of corpus breadth against height (Fig. 4) show that species overlap in height at early ages, but older

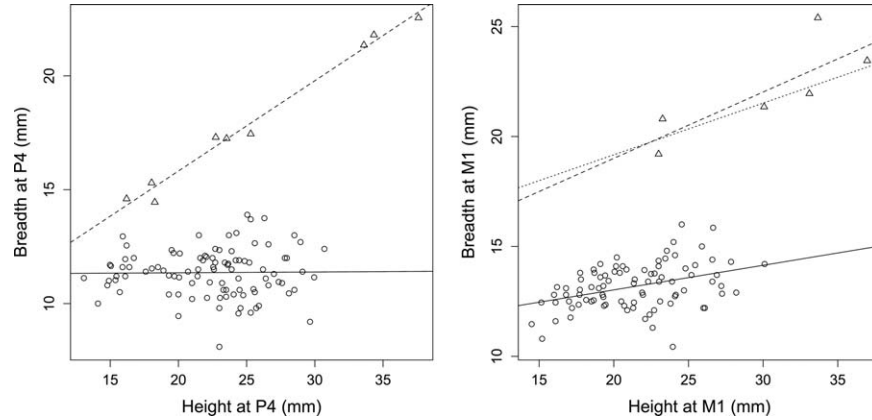


**Fig. 4.** Corpus breadth-height (robusticity) allometry. The left plot is at the position of  $P_4$  and the right is at  $M_1$ . Humans are circles and *A. robustus* are triangles, with least squares regression lines passing through each. For robusticity at  $M_1$ , *A. robustus* has two regression lines, the dashed including all specimens preserving both height and breadth, and the dotted omitting the extremely broad SKW 5.

TABLE 5. Summary of regression analyses for corpus breadth against corpus height at  $P_4$  and  $M_1$

Position	Species	Slope	Intercept	RSE	$R^2$	$P$ value
$P_4$	Human	0.003	11.3	1.04	0.0002	0.892
	<i>A. robustus</i>	0.397	7.89	0.408	0.985	$1.13 \times 10^{-7}$
$M_1$	Human	0.112	10.8	0.951	0.147	0.0002
	<i>A. robustus</i>	0.302	13.0	1.44	0.646	0.054
	<i>A. robustus</i> (no SKW5)	0.235	14.5	0.685	0.855	0.025

Because SKW 5 is extremely broad at the position of  $M_1$ , the regression of breadth against height was computed both with and without this specimen. RSE = Residual standard error.

adolescent *A. robustus* exceed the human range. *A. robustus* corpus breadth, however, is always above the human range, so that at a given age and corpus height, the *A. robustus* corpus is always relatively broader than humans. In humans, breadth is essentially constant (at  $P_4$ ) or increases modestly ( $M_1$ ) throughout ontogeny, whereas in *A. robustus* it is always steadily increasing (Table 5). Although robusticity decreases with age and corpus height in each species (i.e., slope  $< 1$ ), the decrease is slower in *A. robustus* than in humans. Thus, species can be distinguished in robusticity from the earliest ages, and the broad adult *A. robustus* corpus is achieved by relatively slower loss of robusticity compared with humans. In addition, whereas there is great overlap in height and breadth between eruption stages in humans, in *A. robustus* there is a notable size increase in both (especially height) between eruption Stages 3–4.

## DISCUSSION

This study examined how the unique size and shape of the *A. robustus* mandible came about through growth and development. This study focused on relative size change, the proportional size difference between different eruption stages, rather than on growth rates per se (i.e., mm per year). Histological studies of crown formation times suggest more rapid development in australopithecines than in humans (Beynon and Dean, 1988; Dean et al., 1993; LaCruz et al., 2006, 2008), implying that the eruption stages used in this study would have been reached at younger ages in *A. robustus*. Thus, actual

absolute growth rates for most dimensions would likely have been greater in *A. robustus* than they are in modern humans, helping the former attain a massive overall size (Figs. 2–5).

Although some aspects of the *A. robustus* mandibular shape were probably established prenatally, the present results highlight the importance of postnatal growth in creating characteristic *A. robustus* mandibular anatomy. Both the resampling and allometric analyses reveal the development of corpus robusticity. In humans, there is much overlap in breadth between different eruption stages, whereas older stages are generally elevated over earlier ones in *A. robustus* (Figs. 3 and 4). This breadth increase is most notable between eruption Stages 1–2 and 3–4. One mechanism for this difference is the persistence of the ramus root on the lateral corpus as the jaw grows anteriorly in *A. robustus*. In eruption Stage 1, the root flanks the  $dm_2$  in both species. By Stage 2 the root is usually positioned more posteriorly in humans to flank the erupting  $M_1$ , and then the distal  $M_1$  by Stage 3. However, in *A. robustus* the root contributes to corpus breadth at the  $dm_2$  up to Stage 3. Not only is the *A. robustus* ramus root generally more anteriorly positioned than in humans of comparable dental eruption but it is also mediolaterally broader, reflected by a wide extramolar sulcus even at young ages (Bromage, 1989; White, 1977).

Some aspects of the species differences in mandibular growth may be due at least in part to disparate tooth sizes. On the one hand, significantly greater corpus breadth growth in *A. robustus* around  $P_4$ – $M_1$  in early stages likely reflects the development of megadont



postcanine teeth. The premolar crowns either have only begun to form ( $P_3$ ) or are absent ( $P_4$ ) in Stage 1, but are more fully formed in Stage 2 (Conroy and Vannier, 1991). On the other hand, the corpus continues to broaden throughout ontogeny, even at more anterior positions where tooth crowns and roots are already formed. A possible explanation for this discrepancy is that this anterior corpus broadening may be residual to thickening occurring posteriorly to accommodate the later developing  $M_{2-3}$ .

Species differences in the growth of anteroposterior dimensions are also likely related to the large postcanine teeth of *A. robustus*. Between Stages 3–4 *A. robustus* shows markedly greater increase in the distance from the mental foramen to the end of the lingual tuberosity (Trait 21). The lingual tuberosity of the only *A. robustus* in stage 3 (SK 63) encloses a partially developed  $M_2$  crown, and there is no hint of  $M_3$  crown formation distally (Mann, 1975; Conroy and Vannier, 1991). By eruption Stage 4, the *A. robustus* lingual tuberosity has extended posteriorly to surround a developing  $M_3$  crown in all but one specimen (SK 25, the smallest, least mature, and presumably youngest in stage 4). This dimension also increases more in *A. robustus* between Stages 1–2, concomitant with the beginning of  $M_2$  crown formation (Conroy and Vannier, 1991), although the species difference is neither significant nor as marked as between Stages 3–4. These results are consistent with the findings of Boughner and Dean (2004) in *Pan* and *Papio* mandibles, that the length of the corpus always provided “excess” crypt space distal to the mineralizing molar crowns, and that posterior corpus length increased most when the  $M_3$  crown began to mineralize.

The development of teeth of different sizes is one mechanism at least partially responsible for the species differences in mandibular growth identified here. An additional explanation, not necessarily mutually exclusive, is that extreme corpus breadth growth in *A. robustus* may be an adaptive response to processing a hard diet (i.e., Grine et al., 2012) during the growth period. However, biomechanical inferences, especially related to ontogeny, must be made cautiously. Daegling (1989, 1996) warned that anatomical differences between African apes do not necessarily correspond to significant biomechanical differences. Taylor (2002) later confirmed that not all differences in shape (and ontogenetic shape change) between African apes were fully predictable from their dietary differences. Daegling (1989, 2007) has also shown that raw corpus breadth measures and the “robusticity index” (breadth/height) are poor predictors of strength against torsion and bending, stressing that the distribution of cortical bone about a cross-section is key to determining strength. Thus, direct assessment of corpus cross-sections and cortical bone distributions for this sample are necessary to test the hypothesis that extreme and rapid corpus breadth increase was an adaptive response to masticatory loading during *A. robustus* ontogeny.

It has also been hypothesized that the tall vertical ramus and posterior face in *A. robustus* was a result of more extreme facial growth rotation than in other hominoids (Bromage, 1989; McCollum, 1997, 1999). A corollary of such rotation is greater increase in posterior than anterior facial height (Björk and Skieller, 1972; Karlson, 1997; Wang et al., 2009), and the fact that mean grdif is greater for ramus (Trait 28) than symphysis height (Trait 18) across all possible comparisons is

consistent with this hypothesis. While the present results are suggestive, angular data describing corpus-ramus relationships may be more appropriate to test the hypothesis of greater facial rotation in *A. robustus*.

Results also hint that *A. robustus* lacked an adolescent growth spurt in height, something argued to be unique to modern humans among living hominoids (Bogin, 1999). Whether such a spurt was present in early hominins is debatable (e.g., Antón and Leigh, 2003). In humans, several measurements of mandibular height or length have been shown to undergo a growth spurt close in time and relative intensity as the spurt in stature (Bergersen, 1972; Franchi et al., 2000). Importantly, the period in which most height measures experience greatest size increase in *A. robustus* is between Stages 3–4. In contrast, grdif statistics for height are generally more negative between Stages 4–5, indicating greater size change (though not significantly) in humans during this period. Interestingly, in a geometric morphometric study of skull growth in humans and chimpanzees, Bastir and Rosas (2004) found a similar species difference in patterns of size change (i.e., their Fig. 1C). Chimpanzee mandibular size increased most between the occlusion of  $M_1$  and  $M_2$  (Stages 3–4 here) whereas human mandibular size increased more between occlusion of  $M_2$  and  $M_3$  (Stages 4–5 here). While the present findings are suggestive about growth and life history in *A. robustus*, further analysis of the mandibular correlates of body size growth in humans and other hominoids (e.g., Cofran, 2014) is necessary to definitively rule out a growth spurt in stature for this fossil species.

The present study identified how *A. robustus* mandibular size and shape came about through growth. Because of the small size and fragmentary nature of the fossil sample, a resampling procedure was introduced to facilitate understanding of ontogenetic variation in the *A. robustus* mandible, by comparison with a larger sample of modern humans. Species differences in the amount of size growth are consistent with expectations based on anatomical differences between adults. The timing of major differences coincides first with the beginning of permanent tooth eruption (between Stages 1–2) and second with the eruption of  $M_2$  (between Stages 3–4). Greater size increase for many dimensions in *A. robustus* can be attributed to the development of their large postcanine teeth. However, not all species differences in growth can be so easily attributed, and may relate to biomechanical adaptation or the timing of growth spurts. While further analyses are required to test these hypotheses, results presented here point to an important role for postnatal growth in establishing the unique mandibular anatomy of *A. robustus*, and further provide a basis for analyzing mandibular ontogeny in other early hominins with smaller sample sizes.

## ACKNOWLEDGMENTS

I am very grateful to Stephany Potze, Lazarus Kgasi, and Tersia Perregil at the Ditsong National Museum of Natural History in Pretoria, and to Richard Meindl and Mary Ann Raghanti at Kent State University in Ohio for access to collections. Research at KSU furthermore would not have been possible without the hospitality of Caroline Tannert and Aidan Ruth. This work benefited from comments and suggestions from his PhD committee: Milford Wolpoff, Laura MacLachy, Adam Van Arsdale, and Eric Hetland. Adam Van Arsdale was especially crucial in

helping him develop the resampling algorithms, and provided very helpful comments on an earlier version of this article. Comments and suggestions from Frank Williams and an anonymous reviewer greatly improved the content and quality of this article. This work was supported in part by grants from the International Institute and the African Studies Center at the University of Michigan.

### LITERATURE CITED

- Ackermann RR, Krovitz GE. 2002. Common patterns of facial ontogeny in the hominid lineage. *Anat Rec* 269:142–147.
- Alberch P, Gould SJ, Oster GF, Wake DB. 1979. Size and shape in ontogeny and phylogeny. *Paleobiology* 5:296–317.
- Antón SC, Leigh SR. 2003. Growth and life history in *Homo erectus*. In: Thompson JL, Krovitz GE, Nelson AJ, editors. *Patterns of growth and development in the genus Homo*. Cambridge: Cambridge University Press. p 219–245.
- Bastir M, Rosas A. 2004. Comparative ontogeny in humans and chimpanzees: similarities, differences, and paradoxes in postnatal growth and development of the skull. *Ann Anat* 186: 503–509.
- Bergersen EO. 1972. Male adolescent facial growth spurt: its prediction and relation to skeletal maturation. *Angle Orthod* 42:319–338.
- Beynon AD, Dean MC. 1988. Distinct dental developmental patterns in early fossil hominids. *Nature* 335:509–514.
- Björk A, Skieller V. 1972. Facial development and tooth eruption: an implant study at the age of puberty. *Am J Orthod* 62: 339–383.
- Bogin B. 1999. Evolutionary perspective on human growth. *Annu Rev Anthropol* 28:109–153.
- Boughner JC, Dean MC. 2004. Does space in the jaw influence the timing of molar crown initiation? A model using baboons (*Papio anubis*) and great apes (*Pan troglodytes*, *Pan paniscus*). *J Hum Evol* 46:255–277.
- Braga J. 1998. Chimpanzee variation facilitates the interpretation of the incisive suture closure in South African Plio-Pleistocene hominids. *Am J Phys Anthropol* 135:121–135.
- Bromage TG. 1989. Ontogeny of the early hominid face. *J Hum Evol*:751–773.
- Cobb SN, O'Higgins P. 2004. Hominins do not share a common postnatal facial ontogenetic shape trajectory. *J Exp Zool B Mol Dev Evol* 321:302–321.
- Cofran ZC. 2014. Mandibular correlates of body size in chimpanzees and gorillas [abstract]. *Am J Phys Anthropol* S58:95.
- Conroy GC, Vannier MW. 1991. Dental development in South African australopithecines. Part II: dental stage assessment. *Am J Phys Anthropol* 86:137–156.
- Daegling DJ. 1989. Biomechanics of cross-sectional size and shape in the hominoid mandibular corpus. *Am J Phys Anthropol* 80:91–106.
- Daegling DJ. 1996. Growth in the mandibles of African apes. *J Hum Evol* 30:315–341.
- Daegling DJ. 2007. Morphometric estimation of torsional stiffness and strength in primate mandibles. *Am J Phys Anthropol* 132:261–266.
- Daegling DJ, Grine FE. 1991. Compact bone distribution and biomechanics of early hominid mandibles. *Am J Phys Anthropol* 86:321–339.
- Daegling DJ, Hylander WL. 2000. Experimental observation, theoretical models, and biomechanical inference in the study of mandibular form. *Am J Phys Anthropol* 112:541–551.
- Dahlberg AA, Menegaz-Bock RM. 1958. Emergence of the permanent teeth in Pima Indian children. *J Dent Res* 17:1123–1140.
- Dean MC. 1988a. Growth of teeth and development of the dentition in *Paranthropus*. In: Grine FE, editor. *Evolutionary history of the "robust" australopithecines*. New York: Transaction Publishers. p 43–53.
- Dean MC. 1988b. Growth processes in the cranial base of hominoids and their bearing on morphological similarities that exist in the cranial base of *Homo* and *Paranthropus*. In: Grine FE, editor. *Evolutionary history of the "robust" australopithecines*. New York: Transaction Publishers. p 107–112.
- Dean MC, Beynon AD, Thackeray JF, Macho GA. 1993. Histological reconstruction of dental development and age at death of a juvenile *Paranthropus robustus* specimen, SK 63, from Swartkrans, South Africa. *Am J Phys Anthropol* 91:401–419.
- Enlow DH, Harris DB. 1964. A study of the postnatal growth of the human mandible. *Am J Orthod* 50:25–50.
- Eveleth PB, Tanner JM. 1988. *Worldwide variation in human growth*. Cambridge: Cambridge University Press.
- Franchi L, Baccetti T, McNamara JA. 2000. Mandibular growth as related to cervical vertebral maturation and body height. *Am J Orthod Dentofacial Orthop* 118:335–340.
- Fukase H, Suwa G. 2008. Growth-related changes in prehistoric Jomon and modern Japanese mandibles with emphasis on cortical bone distribution. *Am J Phys Anthropol* 136:441–454.
- Grine FE, Daegling DJ. 1993. New mandible of *Paranthropus robustus* from Member 1, Swartkrans Formation, South Africa. *J Hum Evol* 24:319–333.
- Grine FE, Sponheimer M, Ungar PS, Lee-Thorp J, Teaford MF. 2012. Dental microwear and stable isotopes inform the paleoecology of extinct hominins. *Am J Phys Anthropol* 148:285–317.
- Gunz P. 2012. Evolutionary relationships among robust and gracile australopithecines: an "evo-devo" perspective. *Evol Biol* 32: 472–487.
- Hägg U, Taranger J. 1981. Dental emergence stages and the pubertal growth spurt. *Acta Odontol Scand* 39:295–306.
- Holmes MA, Ruff CB. 2011. Dietary effects on development of the human mandibular corpus. *Am J Phys Anthropol* 145: 615–628.
- Johnson PA, Atkinson PJ, Moore WJ. 1976. The development and structure of the chimpanzee mandible. *J Anat* 122:467–477.
- Karlsen AT. 1997. Association between facial height development and mandibular growth rotation in low and high MP-SN angle faces: a longitudinal study. *Angle Orthod* 67:103–110.
- Lacruz RS, Dean MC, Ramirez-Rozzi F, Bromage TG. 2008. Megadontia, striae periodicity and patterns of enamel secretion in Plio-Pleistocene fossil hominins. *J Anat* 213:148–158.
- Lacruz RS, Ramirez Rozzi F, Bromage TG. 2006. Variation in enamel development of South African fossil hominids. *J Hum Evol* 51:580–590.
- Lieberman DE, Krovitz GE, Yates FW, Devlin M, St. Claire M. 2004. Effects of food processing on craniofacial growth in a retrognathic face. *J Hum Evol* 46:655–677.
- Liversidge HM. 2003. Variation in modern human dental development. In: Thompson JL, Krovitz GE, Nelson AJ, editors. *Patterns of growth and development in the Genus Homo*. Cambridge: Cambridge University Press. p 73–1113.
- Lockwood CA, Menter CG, Moggi-Cecchi J, Keyser AW. 2007. Extended male growth in a fossil hominin species. *Science* 318:1443–1446.
- Lovejoy CO, Meindl RS, Pryzbeck TR, Barton TJ, Heiple KG, Kottling D. 1977. Paleodemography of the Libben Site, Ottawa County, Ohio. *Science* 198:291–293.
- Manly BF. 2007. *Randomization, bootstrap and Monte Carlo methods in biology*, 3rd ed. Boca Raton: Chapman & Hall/CRC.
- Mann A. 1975. *Some Paleodemographic Aspects of the South African Australopithecines*. Philadelphia: University of Pennsylvania Publications.
- Mattfeldt T. 2011. A brief introduction to computer-intensive methods, with a view towards applications in spatial statistics and stereology. *J Microsc* 242:1–9.
- McCollum MA. 1997. Palatal thickening and facial form in *Paranthropus*: examination of alternative developmental models. *Am J Phys Anthropol* 103:375–392.
- McCollum MA. 1999. The robust australopithecine face: a morphogenetic perspective. *Science* 284:301–305.
- McCollum MA. 2008. Nasomaxillary remodeling and facial form in robust *Australopithecus*: a reassessment. *J Hum Evol* 54: 2–14.

- McNulty KP. 2012. Evolutionary development in *Australopithecus africanus*. *Evol Biol* 39:488–498.
- McNulty KP, Frost SR, Strait DS. 2006. Examining affinities of the Taung child by developmental simulation. *J Hum Evol* 51:274–296.
- Meindl RS, Mensforth RP, Lovejoy CO. 2008. The Libben site: a hunting, fishing, and gathering village from the eastern Late Woodlands of North America. Analysis and implications for paleodemography and human origins. In: Bocquet-Appel J-P, editor. *Recent advances in paleodemography*. Dordrecht: Springer. p 259–275.
- Mitteroecker P, Gunz P, Bernhard M, Schaefer K. 2004. Comparison of cranial ontogenetic trajectories among great apes and humans. *J Hum Evol* 46:679–698.
- Mitteroecker P, Gunz P, Bookstein FL. 2005. Heterochrony and geometric morphometrics: a comparison of cranial growth in *Pan paniscus* versus *Pan troglodytes*. *Evol Dev* 7:244–258.
- Pickering R, Kramers JD, John P, De Ruiter DJ, Woodhead JD. 2011. Contemporary flowstone development links early hominin bearing cave deposits in South Africa. *Earth Planet Sci Lett* 306:23–32.
- Ponce de Leon MS, Zollikofer CP. 2001. Neandertal cranial ontogeny and its implications for late hominid diversity. *Nature* 412:534–538.
- R Core Team. 2013. R: A language and environment for statistical computing. Vienna: R Foundation for Statistical Computing.
- Rak Y. 1983. *The australopithecine face*. New York: Academic Press.
- Rak Y, Hylander WL. 2008. What else is the tall mandibular ramus of the robust australopithecids good for? In: Vinyard C, Ravosa MJ, Wall C, editors. *Primate craniofacial function and biology*. Boston: Springer. p 431–442.
- Richtsmeier JT, Lele SR. 1993. A coordinate-free approach to the analysis of growth patterns: models and theoretical considerations. *Biol Rev* 68:381–411.
- Richtsmeier JT, Walker A. 1993. A morphometric study of facial growth. In: Walker A, Leakey R, editors. *The Nariokotome Homo erectus skeleton*. Cambridge: Harvard University Press. p 391–420.
- Robinson JT. 1954. Prehominid dentition and hominid evolution. *Evolution* 8:324–334.
- Shea BT. 1983. Allometry and heterochrony in the African apes. *Am J Phys Anthropol* 62:275–289.
- Skinner MF. 1978. Dental maturation, dental attrition and growth of the skull in fossil Hominidae. PhD thesis. Cambridge: Cambridge University.
- Smith BH. 1986. Dental development in *Australopithecus* and early *Homo*. *Nature* 323:327–330.
- Strand Viðarsdóttir U, O’Higgins P, Stringer CB. 2002. A geometric morphometric study of regional differences in the ontogeny of the modern human facial skeleton. *J Anat* 201:211–229.
- Taylor AB. 2002. Masticatory form and function in the African apes. *Am J Phys Anthropol* 117:133–156.
- Teaford MF, Ungar PS. 2000. Diet and the evolution of the earliest human ancestors. *Proc Nat Acad Sci USA* 97:13506–13511.
- Tompkins RL. 1996. Relative dental development of Upper Pleistocene hominids compared to human population variation. *Am J Phys Anthropol* 99:103–118.
- Van Arsdale AP. 2006. Mandibular variation in early *Homo* from Dmanisi, Georgia. PhD thesis. Ann Arbor, MI: University of Michigan.
- Van Arsdale AP, Lordkipanidze D. 2012. A quantitative assessment of mandibular variation in the Dmanisi Hominins. *PaleoAnthropol* 2012:134–144.
- Wang MK, Buschang PH, Behrents R. 2009. Mandibular rotation and remodeling changes during early childhood. *Angle Orthod* 79:271–275.
- White TD. 1977. The anterior mandibular corpus of early African hominidae: functional significance of shape and size. PhD thesis. Ann Arbor, MI: University of Michigan.
- Williams FL, Godfrey LR, Sutherland MR. 2003. Diagnosing heterochronic perturbations in the craniofacial evolution of *Homo* (Neandertals and modern humans) and *Pan* (*P. troglodytes* and *P. paniscus*). In: Thompson J, Krovitz G, Nelson A, editors. *Patterns of growth and development in the genus Homo*. Cambridge: Cambridge University Press. p 295–319.
- Wolpoff MH. 1975. Some aspects of human mandibular evolution. In: McNamara JA, editor. *Determinants of mandibular form and growth*. Ann Arbor: Center for Human Growth and Development, University of Michigan. p 1–64.
- Wolpoff MH. 1979. The Krapina dental remains. *Am J Phys Anthropol* 50:67–114.
- Wolpoff MH. 1999. *Paleoanthropology*, 2nd ed. Boston: McGraw-Hill.
- Wood BA, Aiello LC. 1998. Taxonomic and functional implications of mandibular scaling in early hominins. *Am J Phys Anthropol* 105:523–538.
- Zollikofer CP, Ponce de León MS. 2004. Kinematics of cranial ontogeny: heterotopy, heterochrony, and geometric morphometric analysis of growth models. *J Exp Zool B Mol Dev Evol* 302:322–340.